HHS Public Access

Author manuscript

Neurobiol Aging. Author manuscript; available in PMC 2022 December 01.

Published in final edited form as:

Neurobiol Aging. 2022 December ; 120: 105–116. doi:10.1016/j.neurobiolaging.2022.08.013.

Functional connectivity to the premotor cortex maps onto longitudinal brain neurodegeneration in progressive apraxia of speech

Irene Sintini, PhD[1], **Joseph R. Duffy, PhD**[2], **Heather M. Clark, PhD**[2], **Rene L. Utianski, PhD**[2], **Hugo Botha, MD**[2], **Mary M. Machulda, PhD**[3], **Matthew L. Senjem, MS**[4], **Edythe A. Strand, PhD**[2,5], **Christopher G. Schwarz, PhD**[1], **Val. J. Lowe, MD**[1], **Clifford R. Jack Jr, MD**[1], **Keith A. Josephs, MD**[2], **Jennifer L. Whitwell, PhD**[1]

[1]Department of Radiology, Mayo Clinic, Rochester, MN

[2]Department of Neurology, Mayo Clinic, Rochester, MN

[3]Department of Psychiatry and Psychology, Mayo Clinic, Rochester, MN

[4]Department of Information Technology, Mayo Clinic, Rochester, MN

[5]Department of Speech & Hearing Sciences, University of Washington, Seattle, WA, USA

Abstract

Primary progressive apraxia of speech (PPAOS) is a neurodegenerative motor speech disorder affecting the ability to produce speech. If agrammatic aphasia is present, it can be referred to as the non-fluent/agrammatic variant of primary progressive aphasia (nfvPPA). We investigated whether resting-state functional MRI (rs-fMRI) connectivity from disease 'epicenters' correlated with longitudinal grey matter atrophy and hypometabolism in nfvPPA and PPAOS. Eighteen nfvPPA and 23 PPAOS patients underwent clinical assessment, structural MRI, rs-fMRI, and [^{18}F] fluorodeoxyglucose (FDG)-PET at baseline and ~2 years follow-up. Rates of neurodegeneration in nfvPPA and PPAOS correlated with functional connectivity to the premotor, motor, and frontal cortex. Connectivity to the caudate and thalamus was more strongly associated with rates of hypometabolism than atrophy. Connectivity to the left Broca's area was more strongly associated with rates of atrophy and hypometabolism in nfvPPA. Finally, functional connectivity to a network of regions, and not to a single epicenter, correlated with rates of neurodegeneration in PPAOS and nfvPPA, suggesting similar biological mechanisms driving disease progression, with regional differences related to language.

Keywords

aphasia; apraxia of speech; functional connectivity; multimodal imaging; longitudinal neurodegeneration

Correspondence to Irene Sintini, Ph.D., Mayo Clinic, 200 1st St. SW, Rochester, MN 55905, USA, sintini.irene@mayo.edu.

Supplementary material

Supplementary material associated with this article can be found in the online version.

1. Introduction

Primary progressive apraxia of speech (PPAOS) is a neurodegenerative motor speech disorder which affects the ability to produce speech that is phonetically or prosodically normal (Josephs, Duffy, Stand, et al. 2012; Josephs, Duffy, Strand, et al. 2012). Patients with PPAOS have an isolated apraxia of speech (AOS) with no unequivocal evidence of aphasia. If agrammatic aphasia is present, this syndrome is referred to as the non-fluent/agrammatic variant of primary progressive aphasia (nfvPPA) (Gorno-Tempini et al. 2011) or apraxia of speech with progressive agrammatic aphasia (AOS-PAA). PPAOS is associated with volume loss on MRI and hypometabolism on [^{18}F] fluorodeoxyglucose PET limited to the medial and lateral premotor cortex (Josephs et al. 2021; Josephs et al. 2014; Josephs, Duffy, Strand, et al. 2012), while nfvPPA is associated with additional involvement of inferior and middle frontal gyri, particularly on the left, motor cortex and basal ganglia (Caso et al. 2014; Whitwell, Duffy, et al. 2017; Routier et al. 2018). Increased rates of neurodegeneration are also observed across these regions longitudinally (Tetzloff, Duffy, Clark, et al. 2018; Josephs et al. 2021; Josephs et al. 2014; Brambati et al. 2015). The left Broca's area is affected by the disease process in nfvPPA and progressive agrammatic aphasia (PAA) patients, but it has been shown to be more related to agrammatic aphasia than apraxia of speech (Whitwell et al. 2013; Tetzloff, Duffy, Clark, et al. 2018; Mandelli et al. 2016; Tetzloff et al. 2019; Whitwell, Weigand, et al. 2017; Josephs et al. 2013; Flinker et al. 2015; Carbo et al. 2021). With disease progression, the left Broca's area can become involved in PPAOS too (Tetzloff, Duffy, Clark, et al. 2018; Whitwell, Duffy, et al. 2017). Pathologically, nfvPPA and PPAOS are most commonly associated with a 4-repeat (4R) tauopathy (Josephs et al. 2021).

We have shown that supplementary motor area functional and structural connectivity is disrupted in PPAOS and nfvPPA (Botha et al. 2018; Carbo et al. 2021), and the structural connectivity breakdown in PAA in isolation is different from PPAOS and nfvPPA (Carbo et al. 2021). A previous study reported that the left inferior frontal gyrus pars opercularis was the most atrophic region in nfvPPA and connectivity from this region predicted atrophy in functionally and structurally connected regions of the brain (Mandelli et al. 2016). The concept of regions affected by neurodegeneration early in the disease course acting as "epicenters" for the spreading of the pathology in the entire brain has been explored in Alzheimer's disease (Sintini, Graff-Radford, et al. 2021; Franzmeier et al. 2020; Zhou et al. 2012) and primary 4R tauopathies (Franzmeier et al. 2022). A complementary explanation to the intertwined relationship between neurodegeneration and brain networks is offered by the cascade network failure hypothesis (Jones et al. 2016; Jones et al. 2017), which predicts that tau accumulation is associated with network failure and its spatial patterns vary with the clinical phenotype, within specific functional networks related to the cognitive function impaired. This theory was developed specifically to explain the relationship between tau, amyloid-beta and brain networks in Alzheimer's disease. However, it could be used as a theoretical framework to understand similar mechanisms in other neurodegenerative diseases characterized by pathological protein deposition. According to this framework, we expect similarities in the relationship between tau deposition, and therefore patterns of neurodegeneration, and functional connectivity within networks related to speech, which is

abnormal in both PPAOS and nfvPPA, and differences within networks related to language, such as those encompassing the left Broca's area, since aphasia is present only in nfvPPA.

In this study, we aimed to investigate whether resting-state fMRI functional connectivity from epicenters of neurodegeneration in PPAOS and nfvPPA correlated with longitudinal measures of grey matter atrophy from MRI and hypometabolism from [^{18}F] fluorodeoxyglucose (FDG) PET, and whether differences existed between the two syndromes.

2. Materials and Methods

2.1. Participants

Patients who presented with progressive AOS, either with or without agrammatic aphasia, were recruited by the Neurodegenerative Research Group (NRG) at Mayo Clinic, Rochester, Minnesota, USA between 9/22/2010 and 7/17/2018. All patients underwent detailed neurological, speech and language, and neuropsychological evaluations (Josephs et al. 2021). Patients with concurrent illnesses that could account for speech-language deficits, or meeting criteria for another neurodegenerative syndrome, including the semantic or logopenic variants of primary progressive aphasia (PPA) (Gorno-Tempini et al. 2011; Botha et al. 2015), possible or probable progressive supranuclear palsy (PSP) (Hoglinger et al. 2017) or corticobasal syndrome (CBS) (Armstrong et al. 2013) at first visit were excluded. Patients were diagnosed with PPAOS if AOS was present and there was no unequivocal evidence of aphasia (Josephs, Duffy, Strand, et al. 2012). Patients were diagnosed with nfvPPA if both AOS and agrammatism were present (Botha et al. 2015). Patients may meet criteria for nfvPPA without AOS (Gorno-Tempini et al. 2011), but all patients classified as nfvPPA in the current study had AOS. For this study, we identified PPAOS (n=23) and nfvPPA (n=18) patients who had completed longitudinal follow-up. Of the 23 patients diagnosed as PPAOS at baseline, 8 developed aphasia by the follow-up visit. Identical clinical and imaging assessments were performed at both visits. A cohort of 41 cognitively unimpaired individuals of similar age as the patients was also recruited by the NRG and included in the study for the purpose of comparing general cognitive function.

This study was approved by the Mayo Clinic IRB, and all participants gave consent to participate in the research study.

2.2. Speech and language assessments

The full speech and language battery has been previously published (Josephs, Duffy, Strand, et al. 2012). AOS severity was assessed using the Apraxia of Speech Rating Scale (ASRS) (Strand et al. 2014) version 3.0, which measures the presence and prominence of several clinical features of AOS. The motor speech disorders (MSD) scale (adapted from (Yorkston 1993)) was also used to assess motor speech severity. The Western Aphasia Battery-Revised (WAB) (Kertesz 2007) and Token Test Part V (De Renzi and Vignolo 1962) were used to assess aphasia severity. The short form of the Boston Naming Test (BNT) (Lansing et al. 1999) was used to assess confrontation naming. The speech and language evaluations were video recorded, and diagnoses were rendered by consensus between two or three

speech-language pathologists after reviewing the recorded examination (JRD, HMC, RLU and EAS). The presence of AOS was assessed based on all spoken language tasks of the WAB plus additional speech tasks that included vowel prolongation, speech alternating motion rates (e.g., rapid repetition of 'puhpuhpuh'), speech sequential motion rates (e.g., rapid repetition of 'puhtuhkuh'), word and sentence repetition tasks and a conversational speech sample. The subtype of apraxia of speech (i.e., prosodic, phonetic, mixed) and the presence of dysarthria were also assessed, as previously described (Josephs et al. 2014; Utianski et al. 2018). Agrammatism was judged to be present if function word omissions or syntactic errors were present during the spoken or written WAB picture description task, or in general conversation, or if performance was below expectation on the Token Test. The Northwestern Anagram Test (NAT), a measure of grammatical production integrity (Weintraub et al. 2009), was also performed in ~50% of patients. The Movement Disorders Society Sponsored Revision of the Unified Parkinson's Disease Rating Scale part III (MDS-UPDRS III) (Goetz et al. 2008) was used to assess parkinsonism. The Montreal Cognitive Assessment (MoCA) (Nasreddine et al. 2005) was used to assess general cognitive function. The frontotemporal lobar degeneration (FTLD) – modified version of the Clinical Dementia Rating (CDR) Sum of Boxes (SB) was used to assess functional severity (Knopman et al. 2008). All cognitively unimpaired individuals underwent MoCA and a subset of them underwent MDS-UPDRS III (n=14).

2.3. Image acquisition

All 41 participants (23 PPAOS, 18 nfvPPA) underwent a 3T head MRI protocol at baseline and follow-up that included a magnetization prepared rapid gradient echo (MPRAGE) sequence (TR/TE/TI, 2300/3/900 ms; flip angle 8°, 26-cm field of view; 256×256 in-plane matrix with a phase field of view of 0.94, and slice thickness of 1.2 mm (Jack et al. 2008)) and resting-state gradient echo-planar imaging (TR/TE = 3000/30 ms, 90° flip angle, slice thickness 3.3 mm, in-plane resolution 3.3 mm, and 160 volumes). Participants were instructed to keep their eyes open during the resting-state fMRI scanning. All baseline MRI scans were performed on one of two GE scanners (GE Healthcare, Milwaukee, Wisconsin) with identical protocols. Out of the total 41 participants, 39 (23 PPAOS, 16 nfvPPA) underwent a follow-up MRI scan a median of 1.96 years from baseline (range: 0.96, 3.06) on the same GE scanners. Out of the total 41 participants, 39 participants (21 PPAOS, 18 nfvPPA) underwent baseline and follow-up FDG-PET scans, which were performed with a median interval of 1.97 years (range: 0.94, 2.98). FDG-PET scans were acquired using a PET/CT scanner (GE Healthcare, Milwaukee, Wisconsin or Siemens Healthcare, Erlangen, Germany) operating in 3D mode. Participants were injected with [^{18}F] FDG of approximately 459 MBq (range 367-576 MBq) and, after a 30-minute uptake period, an 8-minute FDG-PET scan was acquired consisting of four 2-minute dynamic frames following a low dose CT transmission scan. Standard corrections were applied. The MRI scans were performed a median of one day from the FDG-PET scans at both baseline and follow-up.

2.4. Image processing

Each PET image was rigidly registered to its corresponding MPRAGE using SPM12 (Wellcome Trust Centre for Neuroimaging, London, UK). Gray matter (GM), white matter (WM) and cerebrospinal fluid (CSF) tissue class probabilities, and spatial normalization

parameters were determined for each MPRAGE using Unified Segmentation in SPM12, with the Mayo Clinic Adult Lifespan Template (MCALT) (https://www.nitrc.org/projects/mcalt/) tissue priors and settings. The FDG-PET images of each participant were coregistered to the corresponding MRI and subsequently spatially normalized to the MCALT template by applying the spatial normalization parameters from the unified segmentation of the MRI and blurred with a 6 mm full width at half maximum kernel for voxel-wise analyses. Annualized rate of change images were generated using tensor-based morphometry with symmetric normalization (TBM-SyN) (Vemuri et al. 2015). Briefly, a symmetric diffeomorphic deformation was computed to warp each subject's follow-up MRI to the baseline MRI image. The log of the determinant of the Jacobian matrix of the deformation was then scaled by the inter-scan interval in years, to get an estimate of the annualized rate of change at each voxel. This annualized log Jacobian image was then masked with a binarized GM mask to generate a voxelwise map of GM atrophy rate for each participant and smoothed with a 6 mm full width at half maximum kernel for voxel-wise analyses. FDG-PET standard uptake value ratios (SUVR) were created by dividing each image by the median uptake in the pons. FDG SUVR rates of change images were created by subtracting the baseline image from the follow-up one and dividing by the year difference. nfvPPA and PPAOS group-average annualized change images were then created from the annualized log Jacobians and the annualized rates of change of FDG SUVR. The Brainnetome atlas, which has 246 regions and has been validated for both structural and functional images, was used for parcellation of each subject's set of images (Fan et al. 2016). Median SUVR in the GM and WM and mean Jacobians in the GM were calculated in each Brainnetome region-of -interest (ROI). The left Broca's area ROI was created by merging the following regions in the inferior frontal gyrus of the Brainnetome atlas: dorsal area 44, caudal area 45, rostral area 45, opercular area 44, ventral area 44. Resting-state fMRI were pre-processed using CONN Toolbox (https://web.conn-toolbox.org/) as described previously (Sintini, Graff-Radford, et al. 2021). Briefly, the pre-processing included: discarding the first 10 volumes to obtain steady-state magnetization, slice time correction, re-alignment and unwarp, outliers detection, segmentation and direct normalization to MNI template space, smoothing using spatial convolution with a Gaussian kernel of 6 mm full width half maximum, nuisance regression (WM and CSF signal; head-motion parameters from the re-alignment step and their first derivatives), and bandpass filtering in the 0.009 – 0.08 Hz frequency. No significant differences were observed across groups (nfvPPA, PPAOS) on the mean six head motion parameters. The functional images were parcellated with the Brainnetome atlas. The mean blood-oxygen-level-dependent (BOLD) time series within each ROI of the atlas was extracted and the Pearson's R correlation coefficients were calculated across all ROI pairs. The association matrices were generated by transforming the R coefficients with the Fisher's R-to-Z transformation.

2.5 Statistical analyses

Comparison of rates of neurodegeneration between PPAOS and nfvPPA— Voxel-based group-average maps and T-score maps from one-sample t-tests in SPM12 were obtained on GM annualized log Jacobian and annualized FDG SUVR change images to assess rates of neurodegeneration. T-score maps from the comparison between PPAOS and nfvPPA were obtained with multiple regression analyses, covarying for age, using

SPM12. SPM12 was also used to assess the influence of the annualized rates of decline in clinical metrics for aphasia (WAB-AQ) and apraxia of speech (MSD score) on the rates of neurodegeneration, with multiple regression analyses, covarying for age; to increase the statistical power, these analyses were performed combining PPAOS and nfvPPA into one group.

Group-average correlations between functional connectivity and rates of neurodegeneration—Pearson's *R* correlation coefficients were calculated between group-average regional longitudinal neurodegeneration measurements and baseline functional connectivity to the epicenters. Each region of the Brainnetome atlas was included in the analyses as a potential epicenter. The epicenters were then defined as the regions whose functionally connectivity led to the highest correlations with the rates of neurodegeneration across all other brain regions. We purposely tested how well functional connectivity from the left Broca's area mapped onto rates of neurodegeneration in nfvPPA and PPAOS, since this region was identified as an epicenter in nfvPPA (Mandelli et al. 2016) and we expect to see differences between nfvPPA and PPAOS. The epicenters identified at the group-level for PPAOS and nfvPPA were then tested at the patient-level, with patient-specific Fisher's *R*-to-*Z* transformed correlations between patient-specific regional rates of neurodegeneration and: 1) patient-specific functional connectivity and 2) group-average functional connectivity. These analyses were performed with the aim of assessing inter-individual variability. Group-level functional connectivity was modeled using two methods. Firstly, group-level ROI-to-ROI functional connectivity values were modeled averaging the *Z*-values connectivity matrices in the PPAOS and nfvPPA groups. Secondly, using a graph theory approach, functional connectivity values were modeled as the mean shortest path to the epicenter using the distance_wei_floyd function of the Brain Connectivity Toolbox (brain-connectivity-toolbox.net) on the group-average Z matrices. Partial correlations were also computed controlling for the Euclidean distance of each ROI to the epicenter. The *p* values of the correlations were compared to the Bonferroni-corrected *p* values, to account for the multiple comparisons problem. We then assessed the effect of the annualized rates of decline in WAB-AQ and MSD score on functional connectivity from the epicenters, with seed-based voxel-level correlations performed in CONN Toolbox. These analyses were performed on the entire cohort of PPAOS and nfvPPA patients to increase statistical power. Analyses on functional connectivity from the left Broca's area were also repeated on the nfvPPA group alone. All analyses were performed in Matlab 2018a (The Mathworks, Inc., Natick, MA, USA).

Autocorrelation in brain quantities—Since brain biological regional quantities suffer from autocorrelation, the group-level *p* values of Pearson's correlations were compared with the exact *p* values derived from 1000 surrogate brain maps with autocorrelated spatial heterogeneity generated with BrainSMASH (Burt et al. 2020). BrainSMASH is used to generate surrogate brain maps that have similar autocorrelation properties to the real brain. These surrogate brain maps were created starting from the group-average regional rates of neurodegeneration of our patients. Then the correlations between real group-average functional connectivity from the epicenters and surrogate regional rates of neurodegeneration were calculated in each surrogate brain. If a 'surrogate' correlation had

an exact *p* value that was smaller than the one of the real correlation, the real correlation was likely a consequence of the autocorrelation that is present in brain quantities, and therefore not trustworthy.

3. Results

3.1. Demographic and clinical findings

Demographic and clinical characteristic of the participants are reported in Table 1. nfvPPA participants scored worse than PPAOS participants on the MoCA ($p<0.001$ at baseline and follow-up), WAB-AQ ($p<0.001$ at baseline and follow-up), Boston Naming Test ($p=0.001$ at baseline and $p<0.001$ at follow-up), Token Test part V ($p=0.001$ at baseline and $p=0.003$ at follow-up), MSD score ($p=0.0101$ at follow-up), FTLD-modified CDR-SB ($p=0.037$ at baseline and $p=0.010$ at follow-up), and NAT ($p=0.001$ at baseline and $p<0.001$ at follow-up). Annualized rates of decline were faster for nfvPPA participants than PPAOS on the MoCA ($p=0.003$), WAB aphasia quotient ($p=0.028$), Token Test V ($p=0.031$) and FTLD-modified CDR-SB ($p=0.010$). nfvPPA had fewer years of formal education than PPAOS ($p=0.029$). Severity of apraxia of speech measured by ASRS version 3.0 did not differ between the two groups. The prevalence of dysarthria did not differ between the two groups either. The prosodic subtype of apraxia of speech was slightly more common in PPAOS than in nfvPPA ($p=0.054$).

Baseline general cognitive function as measured on MoCA did not differ between PPAOS patients and cognitively unimpaired individuals (age=68 (66, 71), 30 females (73%), years of education=16 (14, 18), MoCA=27 (26, 28), MDS-UPDRS III=0 (0,2)). However, PPAOS patients performed significantly worse than cognitively unimpaired individuals on MoCA at the follow-up visit ($p=0.03$). nfvPPA patients performed significantly worse than cognitively unimpaired individuals on MoCA at both time points ($p<0.001$). Both nfvPPA and PPAOS patients performed significantly worse than cognitively unimpaired individuals on MDS-UPDRS III at both time points ($p<0.001$). Age was not significantly different between cognitively unimpaired individuals and patients. Education did not differ between PPAOS and cognitively unimpaired individuals, while it was significantly lower in nfvPPA ($p=0.009$).

3.2. Longitudinal neurodegeneration

Figure 1 shows annualized rates of change of grey matter atrophy from structural MRI (Figure 1A) and metabolism from FDG-PET (Figure 1B) in PPAOS and nfvPPA at the voxel-level and ROI-level. The PPAOS group showed the fastest rates of atrophy in bilateral premotor and motor cortices, particularly in superior gyri. The premotor and motor cortices also showed the fastest rates of atrophy in nfvPPA, although in this group rates of atrophy showed more striking involvement of inferior frontal gyri, prefrontal cortex and parietal lobes. Subcortically, nfvPPA showed the highest rates of atrophy in the left pallidum. Rates of decline in metabolism generally mirrored rates of change in atrophy, with notably stronger involvement of subcortical regions, particularly in nfvPPA. In fact, the thalamus showed the fastest rate of decline in metabolism in nfvPPA. The superior and middle frontal gyri, the precentral gyrus and the caudate also showed fast decline in

metabolism in nfvPPA. Unlike rates of atrophy, rates of decline in metabolism survived FWE correction for multiple comparisons ($p<0.05$) in the one-sample *t*-test in a few regions, namely the left supplementary motor area and bilateral precentral gyrus in PPAOS and the left Broca's area, left precentral gyrus, bilateral supplementary motor area and superior frontal gyrus, left thalamus, left caudate in nfvPPA. Rates of decline in neurodegeneration were in general stronger in nfvPPA than in PPAOS, particularly for hypometabolism. When the two syndromes were compared directly, nfvPPA showed faster rates of atrophy in the cingulum, left precentral, left insula, right supplementary motor area and right superior frontal gyrus (Supplementary Figure 1A) and faster rates of hypometabolism in bilateral superior frontal gyrus, left Broca's area, left precentral, left inferior parietal, left supramarginal regions, left hippocampus and left thalamus (Supplementary Figure 1B). These results did not survive FWE correction for multiple comparison at $p<0.05$. When examining the association between decline in clinical measures of aphasia and apraxia of speech and rates of neurodegeneration, we found that faster rates of decline in WAB-AQ were associated with faster rates of atrophy in the left inferior temporal gyrus and left cingulate (Supplementary Figure 2A) and with faster decline in metabolism in the bilateral inferior frontal and precentral gyri, left superior frontal gyrus, and right superior temporal gyrus (Supplementary Figure 2B), across the entire cohort. Faster rates of decline in MSD score were associated with faster rates of atrophy in the bilateral precentral and paracentral gyri (Supplementary Figure 2A) and faster decline in metabolism in the left thalamus (Supplementary Figure 2B), across the entire cohort.

3.2.1. Functional connectivity to the premotor cortex maps onto longitudinal atrophy—

Functional connectivity of regions located mainly in the bilateral frontal, premotor and motor cortex, but also in the lateral parietal cortex (blue regions in Figure 2A), correlated with rates of atrophy across the rest of the brain in nfvPPA and PPAOS. Functional connectivity to the left dorsolateral Brodmann area 6 of the superior frontal gyrus (i.e., superior premotor cortex) and the left caudal dorsolateral Brodmann area 6 of the precentral gyrus had the strongest correlations with longitudinal atrophy in both nfvPPA ($R=-0.6$ and $R=-0.51$, respectively) (Figure 3A, B) and PPAOS ($R=-0.63$ and $R=-0.67$, respectively) (Figure 3C, D). Modeling functional connectivity as the shortest path to the epicenter led to similar correlations for nfvPPA ($R=0.57$ and $R=0.56$, respectively) (Figure 3A, B) and PPAOS ($R=0.50$ and $R=0.55$, respectively) (Figure 3C, D). A positive correlation indicates that a shorter path to the epicenter is associated with faster rates of neurodegeneration, which are negative. Functional connectivity to these regions still led to the highest correlations with rates of atrophy when controlling for the Euclidean distance from the epicenter (Rd values in Figure 3), indicating that spatial proximity did not entirely explain the association between these quantities. When controlling for the Euclidean distance from the epicenter and modeling connectivity as the shortest path to the epicenter, the regions that led to the highest correlations with rates of atrophy were the precentral gyrus in PPAOS (Rd=0.42) (Figure 3D) and the left rostral area of the superior parietal lobule in nfvPPA (Rd=0.48). All these correlations remained significant ($p<0.05$) when compared to the exact p values derived from BrainSMASH, except for the one between the shortest path to the left superior premotor cortex and the rates of atrophy in PPAOS (Supplementary Table 1). Patient-specific correlations between functional connectivity from either of these

two regions and rates of atrophy were in the expected direction and did not differ between nfvPPA and PPAOS, although showing inter-subject variability (Supplementary Table 2, 3). Even though the left ROIs led to the highest correlations, connectivity from the same regions on the right hemisphere was still strongly correlated with longitudinal atrophy (Figure 2). Regions that were more strongly functionally connected to regions located in the medial temporal, occipital, medial parietal and lateral temporal lobes experienced lower rates of neurodegeneration (red regions in Figure 2). This is in part explained by the fact that such regions are anti-correlated (i.e., have negative functional connectivity) to the frontal, premotor and motor cortex as well as caudate and thalamus (brain renders in Figure 3, 4, and 5). Weaker baseline functional connectivity from the left superior premotor cortex to the bilateral occipital cortex was associated with faster rates of decline in MSD score across the entire cohort (Supplementary Figure 3A). Weaker baseline functional connectivity from the left caudal dorsolateral Brodmann area 6 of the precentral gyrus to the right superior and middle frontal gyri and precuneus was associated with faster rates of decline in WAB-AQ across the entire cohort (Supplementary Figure 3B).

3.2.2. Functional connectivity to the superior frontal cortex, caudate and thalamus maps onto longitudinal hypometabolism—

Rates of hypometabolism correlated with functional connectivity from a similar network of regions as rates of atrophy on the cortex (blue regions in Figure 2B), with the highest correlation found using functional connectivity from the left medial Brodmann area 8 of the superior frontal gyrus (Brainnetome SFG_7_1_L) for both nfvPPA (R=−0.59 and Rd=−0.30, Figure 4A) and PPAOS (R=−0.51, Rd not significant, Figure 4D). However, this correlation was largely driven by spatial proximity in PPAOS, since it was not significant after correcting for Euclidean distance. Modeling functional connectivity as the shortest path to the epicenter led to similar correlations for nfvPPA (R=0.58 and Rd =0.26, Figure 4A) and PPAOS (R=0.45 and Rd not significant, Figure 4D). Patient-specific correlations between functional connectivity from this region and rates of hypometabolism did not differ between nfvPPA and PPAOS (Supplementary Table 2, 3). All correlations remained significant (p<0.05) when compared to the exact p values derived from BrainSMASH, except for the one between the shortest path to the left medial Brodmann area 8 of the superior frontal gyrus and the rates of hypometabolism in PPAOS (Supplementary Table 1). Weaker baseline functional connectivity from left medial Brodmann area 8 of the superior frontal gyrus to the left occipital pole was associated with faster decline in MSD scores across the entire cohort (Supplementary Figure 2C).

Unlike longitudinal atrophy, longitudinal declines in metabolism also correlated strongly with subcortical functional connectivity and shortest path to the epicenter, particularly to the right dorsal caudate (Brainnetome BG_6_5_R) in both nfvPPA (R=−0.56 and R=0.59, respectively) (Figure 4B) and PPAOS (R=−0.49 and R=0.50, respectively) (Figure 4E). These correlations remained significant when controlling for the Euclidean distance from the epicenter (Rd values in Figure 4). Functional connectivity of the left dorsal caudate and the thalamus was also strongly correlated with longitudinal hypometabolism (Figure 2B). When controlling for the Euclidean distance from the epicenter, functional connectivity of the thalamus (Brainnetome Tha_8_7) had the highest correlations with rates

of hypometabolism, specifically the right thalamus for nfvPPA (*R*d=−0.47) (Figure 4C) and the left for PPAOS (*R*d=−0.32) (Figure 4F). Group-level functional connectivity from the right thalamus led to stronger correlations with patient-specific rates of hypometabolism in nfvPPA than in PPAOS patients (p=0.06, Supplementary Table 3). The p values of all these correlations also remained significant when compared to the exact p values derived from BrainSMASH (Supplementary Table 1). When controlling for the Euclidean distance from the epicenter and modeling connectivity as the shortest path to the epicenter, the regions that led to the highest correlations with rates of hypometabolism were the right thalamus in nfvPPA (*R*d=0.42) (Figure 4C) and the pregenual area of the left cingulum in PPAOS (*R*d=0.34). Stronger baseline functional connectivity from the right dorsal caudate to the precuneus was associated with faster rates of decline in MSD score across the entire cohort (Supplementary Figure 3D). Weaker baseline functional connectivity from the left thalamus to the right putamen and caudate was associated with faster rates of decline in WAB-AQ (Supplementary Figure 3E).

3.2.3. Left Broca's connectivity and rates of neurodegeneration—In nfvPPA, regions that were more strongly functionally connected to the left Broca's area had higher rates of grey matter atrophy (*R*=−0.30) (Figure 5A) and hypometabolism (*R*=−0.38) (Figure 5B). The use of the shortest path to the epicenter instead of functional connectivity *Z*-values confirmed this pattern for rates of atrophy (*R*=0.39) and rates of hypometabolism (*R*=0.46) (Figure 5A, B). These correlations remained significant when controlling for Euclidean distance (*R*d values in Figure 5A, B). The p value of all these correlations remained significant when compared to the exact p value derived from BrainSMASH (Supplementary Table 1). The same associations were not found between the rates of atrophy in PPAOS and the functional connectivity *Z*-values from the left Broca's area (Figure 5C). The weak correlations found between the shortest path to the left Broca's area and rates of atrophy and hypometabolism and between functional connectivity and rates of hypometabolism in PPAOS (Figure 5C, D) did not survive Bonferroni's correction and did not remain significant when tested against autocorrelation with BrainSMASH (Supplementary Table 1). The subset of PPAOS that had developed aphasia at the follow-up visit and were therefore diagnosed as nfvPPA (8 patients with follow-up MRI, 7 patients with follow-up FDG-PET) did not show a stronger correlation between left Broca's functional connectivity and rates of neurodegeneration than PPAOS participants who did not progress to nfvPPA. Weaker baseline functional connectivity from the left Broca's area was not associated with rates of change in WAB-AQ or MSD scores in the entire cohort nor in the nfvPPA group alone. At the patient-level, despite high inter-individual variability, we found differences between nfvPPA and PPAOS, with functional connectivity from the left Broca's area leading to stronger correlations with rates of neurodegeneration in nfvPPA than in PPAOS patients (Supplementary Table 2, 3). When using patient-specific functional connectivity, correlations between left Broca's area functional connectivity and patient-specific rates of hypometabolism were stronger in nfvPPA than in PPAOS (p=0.07), although the difference was not statistically significant (Supplementary Table 2). When using group-average functional connectivity, correlations between left Broca's area functional connectivity and patient-specific rates of atrophy and hypometabolism were significantly stronger in nfvPPA than PPAOS (p=0.005 and p=0.036, respectively) (Supplementary Table 3).

4. Discussion

This study showed that functional connectivity to a network of premotor, frontal, motor and subcortical regions was associated with longitudinal rates of neurodegeneration in PPAOS and nfvPPA. Findings were largely concordant when assessing atrophy or decline in metabolism, although functional connectivity to the caudate and thalamus correlated with longitudinal rates of hypometabolism but not with rates of atrophy. Functional connectivity to the left Broca's area was only associated with longitudinal rates of atrophy and hypometabolism in nfvPPA and not in PPAOS. Modeling functional connectivity with *Z*-values or with the graph theory metrics of shortest path to the epicenter led to comparable results. These findings suggest that the disease spreads through a network of functionally connected regions located primarily in the frontal and premotor cortex, with similar findings in nfvPPA and PPAOS, albeit with stronger spread into regions connected to the left Broca's area in nfvPPA. This observation complements our recent findings on abnormalities in the supplementary motor area white matter tracts being present in apraxia of speech patients both with and without agrammatic aphasia (Carbo et al. 2021). However, our analyses cannot demonstrate that functional connectivity disruption causes or precedes in time neurodegeneration.

Our findings concur with our previous MRI and FDG-PET work in which we showed that the premotor cortex bears the brunt of the neurodegeneration in PPAOS and nfvPPA, and hence could be an epicenter (Botha et al. 2015; Josephs, Duffy, Stand, et al. 2012; Josephs et al. 2006; Tetzloff, Duffy, Clark, et al. 2018; Josephs et al. 2021). However, we could not identify one region that stood out as the epicenter of neurodegeneration, but instead a network of regions and it is possible that disrupted connectivity in these regions leads to subsequent neurodegeneration. The epicenters identified in this study, i.e., regions whose functional connectivity strength mapped best onto rates of neurodegeneration in the functionally connected regions throughout the brain, do not necessarily coincide with the starting point of the disease in PPAOS and nfvPPA. In fact, it has been suggested that epicenters evolve in the course of tauopathies (Sintini, Graff-Radford, et al. 2021; Vogel et al. 2020) and a variable percent of regions with the highest level of tau can act as epicenters for the spreading of pathology at the subject-level (Franzmeier et al. 2022). The epicenters that we identified at the group-level exhibited a large amount of variability when tested at the subject-level, as expected, since each patient displays unique patterns of neurodegeneration and disease stage also varys among patients. However, the patient-specific correlations between functional connectivity and rates of neurodegeneration revealed reasonable patterns, with correlations in the expected direction and the most significant differences between the PPAOS and nfvPPA patients involving the left Broca's connectivity.

Longitudinal measures of hypometabolism mapped onto functional connectivity of frontal and subcortical regions, particularly the caudate and thalamus, suggesting a role for these subcortical structures in the evolution of the disease over time. This could be driven by the fact that rates of neurodegeneration in these subcortical structures were greater on FDG-PET compared to MRI. The reason for the difference between FDG-PET and MRI is unclear. Hypometabolism in the left caudate was captured by FDG-PET but not by structural MRI in

Parkinson's disease and it was related to motor symptoms (Albrecht et al. 2019). However, our findings could also reflect a different temporal ordering of hypometabolism and atrophy. It has been suggested that hypometabolism precedes atrophy in Alzheimer's disease and other related dementias (Rodriguez-Oroz et al. 2015; Jack et al. 2010; Gordon et al. 2018; Jagust et al. 2006) and we have previously shown that the caudate, particularly on the right, showed early hypometabolism, but not much atrophy, in a patient diagnosed with PPAOS that was followed over 10 years (Tetzloff, Duffy, Strand, et al. 2018). The left caudate and left thalamus subsequently showed decline in metabolism over time in this patient (Tetzloff, Duffy, Clark, et al. 2018). Hypometabolism from FDG PET discriminated nfvPPA and PPAOS better than atrophy longitudinally, consistently with previous research (Tetzloff, Duffy, Clark, et al. 2018), also showing more widespread associations with faster worsening of aphasia. Finally, one study on nfvPPA reported left Broca's hypometabolism but absent cortical thinning, suggesting that, at early disease stage, only PET might be able to capture neurodegeneration in this region (Routier et al. 2018). Taken together, our findings support the hypothesis of a temporal and spatial disconnection between atrophy and hypometabolism in nfvPPA and PPAOS. Atrophy in subcortical structures was also observed in these patients. The thalamus and striatum showed decline in volume in PAOS patients with corticobasal degeneration (Josephs et al. 2021) and in nfvPPA (Mandelli et al. 2016). In progressive supranuclear palsy, which often shares underlying pathology with PPAOS and nfvPPA, hypometabolism and functional disruption in the caudate and thalamus have been related to worse gait and balance performance, pointing toward the involvement of these structures in motor function (Sintini, Kaufman, et al. 2021; Palmisano et al. 2020; Zwergal et al. 2011; Zwergal et al. 2013). The caudate has been reported as part of the speech network, being functionally connected to the inferior frontal gyrus pars opercularis in healthy subjects (Mandelli et al. 2016). Unlike grey matter volume and metabolism, the deep gray intrinsic connectivity network was not altered in PPAOS patients relative to healthy controls (Botha et al. 2018). However, this does not rule out that functional connectivity from the thalamus and caudate to nearby deep gray regions as well as to frontal regions could be a major route for disease spread. Nevertheless, pinning down the role of the thalamus' functional connectivity is problematic since the thalamus is connected to most cortical and subcortical regions and its role includes mediating the network organization of the central nervous system and controlling connectivity across cortical regions (Shine 2021; Nakajima and Halassa 2017).

nfvPPA showed generally faster rates of atrophy and, particularly, hypometabolism than PPAOS, but similar relationships between such rates and functional connectivity from the same set of cortical and subcortical regions. This is consistent with the fact that hypometabolism is thought to precede atrophy, and nfvPPA patients were significantly more impaired clinically and declined more rapidly over time than PPAOS, despite no significant differences in estimated time from symptom onset, which is only a subjective measurement of disease duration. These findings are also consistent with the observation that rates of atrophy in frontotemporal lobar degeneration accelerate as the disease progresses over time (Staffaroni et al. 2020). From this perspective, nfvPPA patients may show faster rates of neurodegeneration than PPAOS because they represent a more advanced stage of a disease continuum. Together with the fact that a subset of PPAOS patients had developed aphasia at their follow-up visit, these findings suggest that nfvPPA and PPAOS could be

thought of as a disease continuum, in which nfvPPA patients progress more rapidly. This is in line with recent research suggesting that, given the overlapping and heterogeneous clinical features of frontotemporal lobar degeneration syndromes (Murley et al. 2020), a 'transdiagnostic' approach is a more useful framework for understanding the disease than mutually exclusive phenotypes, particularly as the disease progresses over time (Murley et al. 2020). It nonetheless remains important for prognostication and treatment planning to carefully describe patients, using the distinct nomenclature to assist our understanding of the similarities and differences of the two clinical syndromes (Whitwell et al. 2021). In fact, we have shown that PPAOS patients have a better survival rates and lower risk of death than patients who initially present with nfvPPA [AOS-PAA] (Whitwell et al. 2021). From this perspective, PPAOS may be a distinct syndrome from nfvPPA, with a slower disease course. Multimodal imaging studies are already contributing to improve the etiologic diagnosis and prognosis of participants in the PPAOS-nfvPPA continuum (Tetzloff, Duffy, Clark, et al. 2018; Carbo et al. 2021; Whitwell et al. 2013; Whitwell, Weigand, et al. 2017; Josephs et al. 2014; Josephs et al. 2006; Josephs et al. 2013; Mandelli et al. 2016) and across the frontotemporal lobar degeneration syndromes (Illan-Gala et al. 2022; Illan-Gala et al. 2021; Murley et al. 2020; Josephs et al. 2021).

Functional connectivity to the left precentral gyrus strongly correlated with rates of atrophy in both PPAOS and nfvPPA. The left precentral gyrus, which has been associated with speech production (Itabashi et al. 2016), showed faster rates of neurodegeneration in nfvPPA than PPAOS, on both MRI and FDG-PET. Even though the highest correlations with rates of atrophy were identified using functional connectivity from the precentral gyrus and premotor cortex on the left hemisphere, the same regions on the right hemisphere showed comparably strong correlations, in line with previous observation of bilateral involvement of the premotor cortex in PPAOS and nfvPPA [AOS-PAA] (Carbo et al. 2021; Josephs, Duffy, Strand, et al. 2012). Functional connectivity of the left Broca's area correlated with rates of neurodegeneration more strongly in nfvPPA than in PPAOS. This concurs with the fact that the Broca's area is associated with agrammatic aphasia (Whitwell et al. 2013) and is typically spared in patients with PPAOS, at least at baseline (Josephs, Duffy, Strand, et al. 2012). However, when functional connectivity was modeled as the shortest path to the epicenter to the left Broca's area, it did show a weak correlation with rates of atrophy and hypometabolism in PPAOS. Therefore, functional connectivity from the left Broca's area is likely playing a role as driver of the disease in both nfvPPA and PPAOS, and this is consistent with the fact that 8 out of 23 PPAOS patients had developed aphasia at the follow-up visit. Consistently, the left aslant tract, which connects the supplementary motor area to the left Broca's area, has been shown to be disrupted in both nfvPPA [AOS-PAA] and, to a lesser extent, PPAOS (Carbo et al. 2021). The correlations between rates of neurodegeneration and shortest path to the left Broca's epicenter were, however, not significant in PPAOS when compared to the ones obtained from surrogate spatially autocorrelated brain maps. The magnitude of the correlation between rates of atrophy and functional connectivity to left Broca's area in nfvPPA (R~0.3) is comparable to that reported in a previous study on the same syndrome (Mandelli et al. 2016). Consistent with that study, we also found a stronger correlation with rates of atrophy when functional connectivity was modeled as the shortest path to the epicenter instead of Z-values. The correlation we

found between left Broca's functional connectivity and rates of atrophy in nfvPPA was considerably smaller than the correlations we found using epicenters in the premotor cortex (R>0.5). This same study reported that atrophy in their nfvPPA patients progressed into areas that overlap with PPAOS, such as the premotor cortex, and apraxia of speech became more prominent over time (Mandelli et al. 2016). Therefore, it is conceivable that, in patients whose initial symptom was aphasia but with co-occuring apraxia of speech, the disease epicenter might shift from the pars opercularis of the inferior frontal gyrus to other regions of the speech network, such as the premotor cortex. Alternatively, the identified disease epicenters may differ depending on the relative degree of apraxia of speech and agrammatic aphasia present in a cohort. Disease epicenter might also be influenced by the subtype of apraxia of speech (i.e., more prominent articulatory or prosodic disruption), which will be the focus of future investigations. In the current cohort, the prosodic subtype was slightly more common in PPAOS than nfvPPA. This is in line with our findings that PPAOS patients with the prosodic subtype of apraxia of speech demonstrate more focal involvement of the supplementary motor area than the ones with the phonetic subtype, who showed more extended neurodegeneration in the frontal and precentral gyri and insula (Utianski et al. 2018), as we found in nfvPPA in the current study.

In the current cohort of nfvPPA and PPAOS, rates of decline in MSD score, a clinical measure of apraxia severity, correlated with faster rates of atrophy in the precentral and postcentral gyri and faster rates of hypometabolism in the left thalamus, consistently with the clinicopathological description of apraxia of speech (Josephs et al. 2006). A prior study demonstrated that PPAOS participants had reduced connectivity of the right supplementary motor area to the rest of the speech and language network and reduced connectivity in the face, salience and left working memory networks, with supplementary motor area connectivity disruption correlating with apraxia of speech severity (Botha et al. 2018). We found that weaker baseline functional connectivity from the left thalamus to the right putamen and caudate was associated with faster rates of decline in WAB-AQ, a clinical measure of agrammatism. Consistently, we have previously reported that PPAOS patients who developed agrammatic aphasia over time experienced greater rates of atrophy in the thalamus and putamen than PPAOS who did not develop agrammatic aphasia (Whitwell, Duffy, et al. 2017). Disrupted functional connectivity from the left superior frontal and premotor cortex to the occipital cortex correlated with rates of decline in MSD score. This finding may mirror the structural degeneration of the left fronto-occipital fasciculus, which is part of the ventral pathway that regulates semantic processes (Friederici and Gierhan 2013) and deteriorates in patients with nfvPPA (D'Anna et al. 2016; Tetzloff, Duffy, Clark, et al. 2018; Grossman et al. 2013). Rates of decline in WAB-AQ correlated with weaker baseline functional connectivity from the left precentral gyrus to the right superior and middle frontal gyri and precuneus. Decline in WAB-AQ correlated more extensively with rates of hypometabolism in the frontotemporal cortex than with rates of atrophy. These findings are spatially consistent but more contained than findings from our previous study that investigated PPAOS and patients with agrammatic aphasia in isolation (Tetzloff, Duffy, Clark, et al. 2018). This is expected, as WAB-AQ captures the core clinical symptom of PAA patients, which is aphasia. PAA patients were not included in this study, which focuses on apraxia of speech. The left Broca's area has been shown to be more involved in the

neurodegeneration process in PAA patients than PPAOS, with faster rates of atrophy and hypometabolism (Tetzloff, Duffy, Clark, et al. 2018) and disruption of the white matter tracts connecting it to the supplementary motor area (Carbo et al. 2021). We have recently shown that PPAOS patients showed the greatest abnormalities in tracts near the supplementary motor area, while PAA patients showed greater disruption in the left prefrontal tract and frontal aslant tract, further away from the supplementary motor area, hinting that the two syndromes have different disease pathways, at least in relation the language network (Carbo et al. 2021).

The main limitation of this study is the small sample size, due to the relative rarity of these disorders. For this reason, the main analyses of our study were conducted at the group-level, as the aim of the study was to compare nfvPPA and PPAOS. Patient-specific analyses led to lower correlations between functional connectivity from the group-level epicenters and the rates of neurodegeneration, suggesting that there is a high level of variability among patients, particularly in fMRI measures, and more research is needed to develop patient-specific functional connectivity biomarkers. Different levels of dysarthria might have influenced neuroimaging findings. However, in the present cohort, there were no significant differences in dysarthria between PPAOS and nfvPPA. There were instead differences in the prevalence of apraxia of speech subtypes between the two groups: future work will need to investigate how this aspect might affect neuroimaging findings. Additionally, a larger cohort of PPAOS patients who develop aphasia through the course of their disease would provide a more detailed insight into the disease mechanisms. PPAOS and nfvPPA often have an underlying 4R tau pathology due to progressive supranuclear palsy or corticobasal degeneration (Josephs et al. 2021). We hypothesize that examining tau, utilizing a PET ligand that can detect 4R tau, in relation to functional connectivity will be important to understand the disease spreading mechanisms, as it has been recently demonstrated that functional connectivity is associated with tau deposition patterns in 4R tauopathies (Franzmeier et al. 2022). Future studies will need to address whether neurodegeneration in disease epicenters is the cause of subsequent neurodegeneration in functionally connected regions as well as whether functional connectivity merely reflect baseline neurodegeneration relative to healthy controls.

5. Conclusions

In summary, this study provides insight into mechanisms of disease evolution in PPAOS and nfvPPA, highlighting the key role of functional connectivity to the premotor cortex, caudate, thalamus and left Broca’s area, but only when aphasia is present, in mapping onto longitudinal measures of neurodegeneration. These findings also suggest that functional connectivity measures may have prognostic value in these patients and future studies will focus on the clinical utility of resting state fMRI in PPAOS and nfvPPA.

Supplementary Material

Refer to Web version on PubMed Central for supplementary material.

Funding

This study was funded by National Institutes of Health grants R01-DC010367, R01-DC12519 and R01-DC14942.

Competing interest

M.L.S. has owned stocks, within the past 12 months, in Align Technology, Inc., Inovio Pharmaceuticals Inc., LHC Group, Inc., Mesa Laboratories, Inc., and Natus Medical Inc., unrelated to the current study. V.J.L. consults for Bayer Schering Pharma, Piramal Life Sciences, Life Molecular Imaging, Eisai Inc., AVID Radiopharmaceuticals, and Merck Research and receives research support from GE Healthcare, Siemens Molecular Imaging, AVID Radiopharmaceuticals. C.R.J. serves on a scientific advisory board for Eli Lilly & Company, as a speaker for Eisai and on an independent data safety monitoring board for Roche but he receives no personal compensation from any commercial entity. All other authors report no competing interests for this study.

Data availability

Data that support the findings in this study are available from the corresponding author upon reasonable request.

References

Albrecht F, Ballarini T, Neumann J, and Schroeter ML. 2019. 'FDG-PET hypometabolism is more sensitive than MRI atrophy in Parkinson's disease: A whole-brain multimodal imaging meta-analysis', Neuroimage-Clinical, 21.

Armstrong MJ, Litvan I, Lang AE, Bak TH, Bhatia KP, Borroni B, Boxer AL, Dickson DW, Grossman M, Hallett M, Josephs KA, Kertesz A, Lee SE, Miller BL, Reich SG, Riley DE, Tolosa E, Troster AI, Vidailhet M, and Weiner WJ. 2013. 'Criteria for the diagnosis of corticobasal degeneration', Neurology, 80: 496–503. [PubMed: 23359374]

Botha H, Duffy JR, Whitwell JL, Strand EA, Machulda MM, Schwarz CG, Reid RI, Spychalla AJ, Senjem ML, Jones DT, Lowe V, Jack CR, and Josephs KA. 2015. 'Classification and clinicoradiologic features of primary progressive aphasia (PPA) and apraxia of speech', Cortex, 69: 220–36. [PubMed: 26103600]

Botha H, Utianski RL, Whitwell JL, Duffy JR, Clark HM, Strand EA, Machulda MM, Tosakulwong N, Knopman DS, Petersen RC, Jack CR, Josephs KA, and Jones DT. 2018. 'Disrupted functional connectivity in primary progressive apraxia of speech', Neuroimage-Clinical, 18: 617–29. [PubMed: 29845010]

Brambati SM, Amici S, Racine CA, Neuhaus J, Miller Z, Ogar J, Dronkers N, Miller BL, Rosen H, and Gorno-Tempini ML. 2015. 'Longitudinal gray matter contraction in three variants of primary progressive aphasia: A tenser-based morphometry study', Neuroimage-Clinical, 8: 345–55. [PubMed: 26106560]

Burt JB, Helmer M, Shinn M, Anticevic A, and Murray JD. 2020. 'Generative modeling of brain maps with spatial autocorrelation', Neuroimage, 220.

Carbo Adrian Valls, Robert I Reid, Nirubol Tosakulwong, Joseph R Duffy, Heather M Clark, Rene L Utianski, Mary M Machulda, Hugo Botha, Edythe A Strand, and Stephen D Weigand. 2021. "Tractography Analysis of Supplementary Motor Area White Matter Tracts in Progressive Apraxia of Speech and Agrammatic Aphasia." In Annals of neurology, S84–S84. WILEY 111 RIVER ST, HOBOKEN 07030-5774, NJ USA.

Caso F, Mandelli ML, Henry M, Gesierich B, Bettcher BM, Ogar J, Filippi M, Comi G, Magnani G, Sidhu M, Trojanowski JQ, Huang EJ, Grinberg LT, Miller BL, Dronkers N, Seeley WW, and Gorno-Tempini ML. 2014. 'In vivo signatures of nonfluent/agrammatic primary progressive aphasia caused by FTLD pathology', Neurology, 82: 239–47. [PubMed: 24353332]

D'Anna L, Mesulam MM, Thiebaut de Schotten M, Dell'Acqua F, Murphy D, Wieneke C, Martersteck A, Cobia D, Rogalski E, and Catani M. 2016. 'Frontotemporal networks and behavioral symptoms in primary progressive aphasia', Neurology, 86: 1393–99. [PubMed: 26992858]

De Renzi A, and Luigi Amedeo Vignolo. 1962. 'Token test: A sensitive test to detect receptive disturbances in aphasics', Brain: a journal of neurology.

Fan LZ, Li H, Zhuo JJ, Zhang Y, Wang JJ, Chen LF, Yang ZY, Chu CY, Xie SM, Laird AR, Fox PT, Eickhoff SB, Yu CS, and Jiang TZ. 2016. 'The Human Brainnetome Atlas: A New Brain Atlas Based on Connectional Architecture', Cerebral Cortex, 26: 3508–26. [PubMed: 27230218]

Flinker A, Korzeniewska A, Shestyuk AY, Franaszczuk PJ, Dronkers NF, Knight RT, and Crone NE. 2015. 'Redefining the role of Broca's area in speech', Proceedings of the National Academy of Sciences of the United States of America, 112: 2871–75. [PubMed: 25730850]

Franzmeier N, Neitzel J, Rubinski A, Smith R, Strandberg O, Ossenkoppele R, Hansson O, Ewers M, and Adni. 2020. 'Functional brain architecture is associated with the rate of tau accumulation in Alzheimer's disease', Nature Communications, 11.

Franzmeier Nicolai, Brendel Matthias, Beyer Leonie, Slemann Luna, Gabor G Kovacs, Thomas Arzberger, Kurz Carolin, Respondek Gesine, Milica J Lukic, and Davina Biel. 2022. 'Tau deposition patterns are associated with functional connectivity in primary tauopathies', Nature Communications, 13: 1–18.

Friederici AD, and Gierhan SME. 2013. 'The language network', Current Opinion in Neurobiology, 23: 250–54. [PubMed: 23146876]

Goetz CG, Tilley BC, Shaftman SR, Stebbins GT, Fahn S, Martinez-Martin P, Poewe W, Sampaio C, Stern MB, Dodel R, Dubois B, Holloway R, Jankovic J, Kulisevsky J, Lang AE, Lees A, Leurgans S, LeWitt PA, Nyenhuis D, Olanow CW, Rascol O, Schrag A, Teresi JA, Hilten JJ, LaPelle N, and Movement Disorder Soc UPDRS. 2008. 'Movement Disorder Society-Sponsored Revision of the Unified Parkinson's Disease Rating Scale (MDS-UPDRS): Scale Presentation and Clinimetric Testing Results', Movement Disorders, 23: 2129–70. [PubMed: 19025984]

Gordon BA, Blazey TM, Su Y, Hari-Raj A, Dincer A, Flores S, Christensen J, McDade E, Wang GQ, Xiong CJ, Cairns NJ, Hassenstab J, Marcus DS, Fagan AM, Jack CR, Hornbeck RC, Paumier KL, Ances BM, Berman SB, Brickman AM, Cash DM, Chhatwal JP, Correia S, Forster S, Fox NC, Graff-Radford NR, la Fougere C, Levin J, Masters CL, Rossor MN, Salloway S, Saykin AJ, Schofield PR, Thompson PM, Weiner MM, Holtzman DM, Raichle ME, Morris JC, Bateman RJ, and Benzinger TLS. 2018. 'Spatial patterns of neuroimaging biomarker change in individuals from families with autosomal dominant Alzheimer's disease: a longitudinal study', Lancet neurology, 17: 241–50. [PubMed: 29397305]

Gorno-Tempini ML, Hillis AE, Weintraub S, Kertesz A, Mendez M, Cappa SF, Ogar JM, Rohrer JD, Black S, Boeve BF, Manes F, Dronkers NF, Vandenberghe R, Rascovsky K, Patterson K, Miller BL, Knopman DS, Hodges JR, Mesulam MM, and Grossman M. 2011. 'Classification of primary progressive aphasia and its variants', Neurology, 76: 1006–14. [PubMed: 21325651]

Grossman M, Powers J, Ash S, McMillan C, Burkholder L, Irwin D, and Trojanowski JQ. 2013. 'Disruption of large-scale neural networks in non-fluent/agrammatic variant primary progressive aphasia associated with frontotemporal degeneration pathology', Brain and Language, 127: 106–20. [PubMed: 23218686]

Hoglinger G, Respondek G, Stamelou A, Kurz C, Josephs K, Lang A, Mollenhauer B, Muller U, Nilsson C, Whitwell J, Boxer A, Golbe L, and Litvan I. 2017. 'Movement Disorder Society - Clinical Diagnostic Criteria for Progressive Supranuclear Palsy', Movement Disorders, 32.

Illan-Gala I, Falgas N, Friedberg A, Castro-Suarez S, Keret O, Rogers N, Oz D, Nigro S, Quattrone A, Quattrone A, Wolf A, Younes K, Santos-Santos M, Borrego-Ecija S, Cobigo Y, Dols-Icardo O, Llado A, Sanchez-Valle R, Clarimon J, Blesa R, Alcolea D, Fortea J, Lleo A, Grinberg LT, Spina S, Kramer JH, Rabinovici GD, Boxer A, Tempini MLG, Miller BL, Seeley WW, Rosen HJ, and Perry DC. 2021. 'Diagnostic Utility of Measuring Cerebral Atrophy in the Behavioral Variant of Frontotemporal Dementia and Association With Clinical Deterioration', Jama Network Open, 4.

Illan-Gala I, Nigro S, VandeVrede L, Falgas N, Heuer HW, Painous C, Compta Y, Marti MJ, Montal V, Pagonabarraga J, Kulisevsky J, Lleo A, Fortea J, Logroscino G, Quattrone A, Quattrone A, Perry DC, Gorno-Tempini ML, Rosen HJ, Grinberg LT, Spina S, La Joie R, Rabinovici GD, Miller BL, Rojas JC, Seeley WW, and Boxer AL. 2022. 'Diagnostic Accuracy of Magnetic Resonance Imaging Measures of Brain Atrophy Across the Spectrum of Progressive Supranuclear Palsy and Corticobasal Degeneration', Jama Network Open, 5.

Itabashi R, Nishio Y, Kataoka Y, Yazawa Y, Furui E, Matsuda M, and Mori E. 2016. 'Damage to the Left Precentral Gyrus Is Associated With Apraxia of Speech in Acute Stroke', Stroke, 47: 31–36. [PubMed: 26645260]

Jack CR Jr., Lowe VJ, Senjem ML, Weigand SD, Kemp BJ, Shiung MM, Knopman DS, Boeve BF, Klunk WE, Mathis CA, and Petersen RC. 2008. '11C PiB and structural MRI provide complementary information in imaging of Alzheimer's disease and amnestic mild cognitive impairment', Brain, 131: 665–80. [PubMed: 18263627]

Jack CR, Knopman DS, Jagust WJ, Shaw LM, Aisen PS, Weiner MW, Petersen RC, and Trojanowski JQ. 2010. 'Hypothetical model of dynamic biomarkers of the Alzheimer's pathological cascade', Lancet neurology, 9: 119–28. [PubMed: 20083042]

Jagust W, Gitcho A, Sun F, Kuczynski B, Mungas D, and Haan M. 2006. 'Brain imaging evidence of preclinical Alzheimer's disease in normal aging', Annals of neurology, 59: 673–81. [PubMed: 16470518]

Jones D, Knopman D, Gunter J, Graff-Radford J, Vemuri P, Boeve B, Petersen R, Weiner M, and Jack C. 2016. 'Cascading Network Failure across the Alzheimer's Disease Spectrum', Neurology, 86.

Jones DT, Graff-Radford J, Lowe VJ, Wiste HJ, Gunter JL, Senjem ML, Botha H, Kantarci K, Boeve BF, Knopman DS, Petersen RC, and Jack CR. 2017. 'Tau, amyloid, and cascading network failure across the Alzheimer's disease spectrum', Cortex, 97: 143–59. [PubMed: 29102243]

Josephs KA, Duffy JR, Clark HM, Utianski RL, Strand EA, Machulda MM, Botha H, Martin PR, Pham NTT, Stierwalt J, Ali F, Buciuc M, Baker M, De Castro CHF, Spychalla AJ, Schwarz CG, Reid RI, Senjem ML, Jack CR, Lowe VJ, Bigio EH, Reichard RR, Polley EJ, Ertekin-Taner N, Rademakers R, DeTure MA, Ross OA, Dickson DW, and Whitwell JL. 2021. 'A molecular pathology, neurobiology, biochemical, genetic and neuroimaging study of progressive apraxia of speech', Nature Communications, 12.

Josephs KA, Duffy JR, Strand EA, Machulda MM, Senjem ML, Gunter JL, Schwarz CG, Reid RI, Spychalla AJ, Lowe VJ, Jack CR, and Whitwell JL. 2014. 'The evolution of primary progressive apraxia of speech', Brain, 137: 2783–95. [PubMed: 25113789]

Josephs KA, Duffy JR, Strand EA, Machulda MM, Senjem ML, Lowe VJ, Jack CR, and Whitwell JL. 2013. 'Syndromes dominated by apraxia of speech show distinct characteristics from agrammatic PPA', Neurology, 81: 337–45. [PubMed: 23803320]

Josephs KA, Duffy JR, Strand EA, Machulda MM, Senjem ML, Master AV, Lowe VJ, Jack CR, and Whitwell JL. 2012. 'Characterizing a neurodegenerative syndrome: primary progressive apraxia of speech', Brain, 135: 1522–36. [PubMed: 22382356]

Josephs KA, Duffy JR, Strand EA, Whitwell JL, Layton KF, Parisi JE, Hauser MF, Witte RJ, Boeve BF, Knopman DS, Dickson DW, Jack CR, and Petersen RC. 2006. 'Clinicopathological and imaging correlates of progressive aphasia and apraxia of speech', Brain, 129: 1385–98. [PubMed: 16613895]

Josephs K, Duffy J, Stand E, Machulda M, Senjem M, Master A, Lowe V, Jack C, and Whitwell J. 2012. 'Primary Progressive Apraxia of Speech (PAS): A Distinct Neurodegenerative Syndrome', Neurology, 78.

Kertesz Andrew. 2007. 'Western Aphasia Battery--Revised'.

Knopman DS, Kramer JH, Boeve BF, Caselli RJ, Graff-Radford NR, Mendez MF, Miller BL, and Mercaldo N. 2008. 'Development of methodology for conducting clinical trials in frontotemporal lobar degeneration', Brain, 131: 2957–68. [PubMed: 18829698]

Lansing AE, Ivnik RJ, Cullum CM, and Randolph C. 1999. 'An empirically derived short form of the Boston Naming Test', Archives of Clinical Neuropsychology, 14: 481–87. [PubMed: 14590575]

Mandelli ML, Vilaplana E, Brown JA, Hubbard HI, Binney RJ, Attygalle S, Santos-Santos MA, Miller ZA, Pakvasa M, Henry ML, Rosen HJ, Henry RG, Rabinovici GD, Miller BL, Seeley WW, and Gorno-Tempini ML. 2016. 'Healthy brain connectivity predicts atrophy progression in non-fluent variant of primary progressive aphasia', Brain, 139: 2778–91. [PubMed: 27497488]

Murley AG, Coyle-Gilchrist I, Rouse MA, Jones PS, Li W, Wiggins J, Lansdall C, Rodriguez PV, Wilcox A, Tsvetanov KA, Patterson K, Ralph MAL, and Rowe JB. 2020. 'Redefining the multidimensional clinical phenotypes of frontotemporal lobar degeneration syndromes', Brain, 143: 1555–71. [PubMed: 32438414]

Nakajima M, and Halassa MM. 2017. 'Thalamic control of functional cortical connectivity', Current Opinion in Neurobiology, 44: 127–31. [PubMed: 28486176]

Nasreddine ZS, Phillips NA, Bedirian V, Charbonneau S, Whitehead V, Collin I, Cummings JL, and Chertkow H. 2005. 'The montreal cognitive assessment, MoCA: A brief screening tool for mild cognitive impairment', Journal of the American Geriatrics Society, 53: 695–99. [PubMed: 15817019]

Palmisano C, Todisco M, Marotta G, Volkmann J, Pacchetti C, Frigo CA, Pezzoli G, and Isaias IU. 2020. 'Gait initiation in progressive supranuclear palsy: brain metabolic correlates', Neuroimage-Clinical, 28.

Rodriguez-Oroz MC, Gago B, Clavero P, Delgado-Alvarado M, Garcia-Garcia D, and Jimenez-Urbieta H. 2015. 'The Relationship Between Atrophy and Hypometabolism: Is It Regionally Dependent in Dementias?', Current Neurology and Neuroscience Reports, 15.

Routier A, Habert MO, Bertrand A, Kas A, Sundqvist M, Mertz J, David PM, Bertin H, Belliard S, Pasquier F, Bennys K, Martinaud O, Etcharry-Bouyx F, Moreaud O, Godefroy O, Pariente J, Puel M, Couratier P, Boutoleau-Bretonniere C, Laurent B, Migliaccio R, Dubois B, Colliot O, Teichmann M, and CAPP Study Grp. 2018. 'Structural, Microstructural, and Metabolic Alterations in Primary Progressive Aphasia Variants', Frontiers in Neurology, 9.

Shine JM 2021. 'The thalamus integrates the macrosystems of the brain to facilitate complex, adaptive brain network dynamics', Progress in Neurobiology, 199.

Sintini I, Graff-Radford J, Jones DT, Botha H, Martin PR, Machulda MM, Schwarz CG, Senjem ML, Gunter JL, Jack CR, Lowe VJ, Josephs KA, and Whitwell JL. 2021. 'Tau and Amyloid Relationships with Resting-state Functional Connectivity in Atypical Alzheimer's Disease', Cerebral Cortex, 31: 1693–706. [PubMed: 33152765]

Sintini I, Kaufman K, Loushin S, Botha H, Martin P, Senjem M, Reid R, Schwarz C, Jack C, Lowe V, Josephs K, Whitwell J, and Ali F. 2021. 'Neuroimaging associations to gait impairments in progressive supranuclear palsy', Movement Disorders, 36: S256–S57.

Staffaroni AM, Goh SYM, Cobigo Y, Ong E, Lee SE, Casaletto KB, Wolf A, Forsberg LK, Ghoshal N, Graff-Radford NR, Grossman M, Heuer HW, Hsiung GYR, Kantarci K, Knopman DS, Kremers WK, Mackenzie IR, Miller BL, Pedraza O, Rascovsky K, Tartaglia MC, Wszolek ZK, Kramer JH, Kornak J, Boeve BF, Boxer AL, and Rosen HJ. 2020. 'Rates of Brain Atrophy Across Disease Stages in Familial Frontotemporal Dementia Associated With MAPT, GRN, and C9orf72 Pathogenic Variants', Jama Network Open, 3.

Strand EA, Duffy JR, Clark HM, and Josephs K. 2014. 'The apraxia of speech rating scale: A tool for diagnosis and description of apraxia of speech', Journal of Communication Disorders, 51: 43–50. [PubMed: 25092638]

Tetzloff KA, Duffy JR, Clark HM, Strand EA, Machulda MM, Schwarz CG, Senjem ML, Reid RI, Spychalla AJ, Tosakulwong N, Lowe VJ, Jack CR, Josephs KA, and Whitwell JL. 2018. 'Longitudinal structural and molecular neuroimaging in agrammatic primary progressive aphasia', Brain, 141: 302–17. [PubMed: 29228180]

Tetzloff KA, Duffy JR, Clark HM, Utianski RL, Strand EA, Machulda MM, Botha H, Martin PR, Schwarz CG, Senjem ML, Reid RI, Gunter JL, Spychalla AJ, Knopman DS, Petersen RC, Jack CR, Lowe VJ, Josephs KA, and Whitwell JL. 2019. 'Progressive agrammatic aphasia without apraxia of speech as a distinct syndrome', Brain, 142: 2466–82. [PubMed: 31199471]

Tetzloff KA, Duffy JR, Strand EA, Machulda MM, Boland SM, Utianski RL, Botha H, Senjem ML, Schwarz CG, Josephs KA, and Whitwell JL. 2018. 'Clinical and imaging progression over 10 years in a patient with primary progressive apraxia of speech and autopsy-confirmed corticobasal degeneration', Neurocase, 24: 111–20. [PubMed: 29799310]

Utianski RL, Duffy JR, Clark HM, Strand EA, Botha H, Schwarz CG, Machulda MM, Senjem ML, Spychalla AJ, Jack CR, Petersen RC, Lowe VJ, Whitwell JL, and Josephs KA. 2018. 'Prosodic and phonetic subtypes of primary progressive apraxia of speech', Brain and Language, 184: 54–65. [PubMed: 29980072]

Vemuri P, Senjem ML, Gunter JL, Lundt ES, Tosakulwong N, Weigand SD, Borowski BJ, Bernstein MA, Zuk SM, Lowe VJ, Knopman DS, Petersen RC, Fox NC, Thompson PM, Weiner MW, Jack CR, and Alzheimer's Dis Neuroimaging Initi. 2015. 'Accelerated vs. unaccelerated serial MRI based TBM-SyN measurements for clinical trials in Alzheimer's disease', Neuroimage, 113: 61–69. [PubMed: 25797830]

Vogel JW, Iturria-Medina Y, Strandberg OT, Smith R, Levitis E, Evans AC, Hansson O, Alzheimer Dis Neuroimaging Initiat, and Swedish BioFinder Study. 2020. 'Spread of pathological tau proteins through communicating neurons in human Alzheimer's disease', Nature Communications, 11.

Weintraub S, Mesulam MM, Wieneke C, Rademaker A, Rogalski EJ, and Thompson CK. 2009. 'The Northwestern Anagram Test: Measuring Sentence Production in Primary Progressive Aphasia', American Journal of Alzheimers Disease and Other Dementias, 24: 408–16.

Whitwell JL, Duffy JR, Machulda MM, Clark HM, Strand EA, Senjem ML, Gunter JL, Spychalla AJ, Petersen RC, Jack CR, and Josephs KA. 2017. 'Tracking the development of agrammatic aphasia: A tensor-based morphometry study', Cortex, 90: 138–48. [PubMed: 27771043]

Whitwell JL, Duffy JR, Strand EA, Xia R, Mandrekar J, Machulda MM, Senjem ML, Lowe VJ, Jack CR, and Josephs KA. 2013. 'Distinct regional anatomic and functional correlates of neurodegenerative apraxia of speech and aphasia: An MRI and FDG-PET study', Brain and Language, 125: 245–52. [PubMed: 23542727]

Whitwell JL, Martin P, Duffy JR, Clark HM, Utianski RL, Botha H, Machulda MM, Strand EA, and Josephs KA. 2021. 'Survival Analysis in Primary Progressive Apraxia of Speech and Agrammatic Aphasia', Neurology-Clinical Practice, 11: 249–55. [PubMed: 34484892]

Whitwell JL, Weigand SD, Duffy JR, Clark HM, Strand EA, Machulda MM, Spychalla AJ, Senjem ML, Jack CR, and Josephs KA. 2017. 'Predicting clinical decline in progressive agrammatic aphasia and apraxia of speech', Neurology, 89: 2271–79. [PubMed: 29093069]

Yorkston KM. 1993. 'Speech deterioration in amyotrophic lateral sclerosis: Implications for the timing of intervention', Jounal of Medical Speech-Language Pathology, 1: 35–46.

Zhou J, Gennatas ED, Kramer JH, Miller BL, and Seeley WW. 2012. 'Predicting Regional Neurodegeneration from the Healthy Brain Functional Connectome', Neuron, 73: 1216–27. [PubMed: 22445348]

Zwergal A, la Fougere C, Lorenzl S, Rominger A, Xiong G, Deutschenbaur L, Linn J, Krafczyk S, Dieterich M, Brandt T, Strupp M, Bartenstein P, and Jahn K. 2011. 'Postural imbalance and falls in PSP correlate with functional pathology of the thalamus', Neurology, 77: 101–09. [PubMed: 21613601]

Zwergal A, la Fougere C, Lorenzl S, Rominger A, Xiong GM, Deutschenbaur L, Schoberl F, Linn J, Dieterich M, Brandt T, Strupp M, Bartenstein P, and Jahn K. 2013. 'Functional disturbance of the locomotor network in progressive supranuclear palsy', Neurology, 80: 634–41. [PubMed: 23345641]

Highlights

- Functional connectivity correlates with neurodegeneration rates in PPAOS and nfvPPA
- Atrophy, hypometabolism correlate with functional connectivity to premotor cortex
- Hypometabolism correlates with connectivity to caudate and thalamus
- Connectivity to left Broca's area correlates with neurodegeneration in nfvPPA

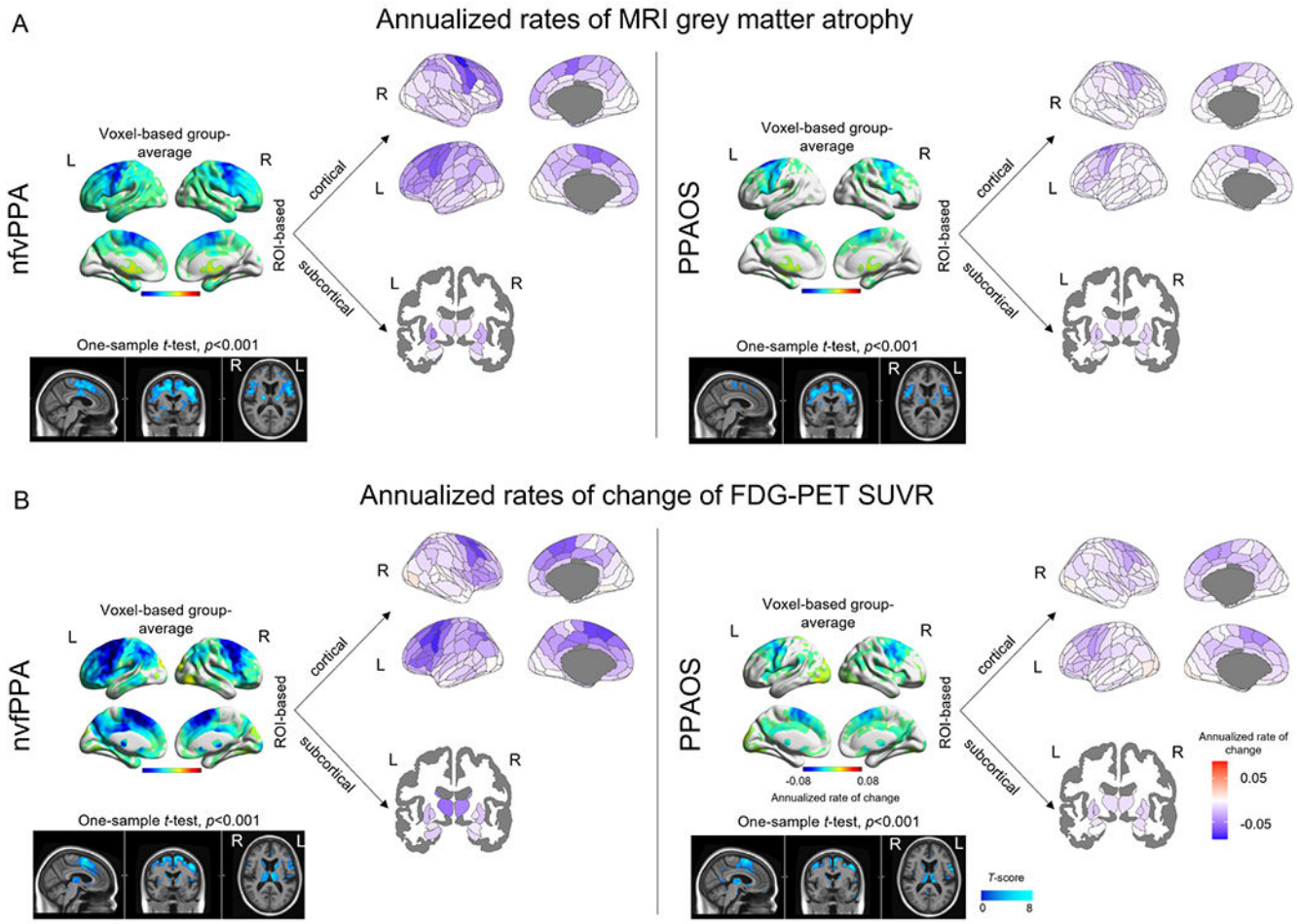

Figure 1. Group-level longitudinal neurodegeneration.

Group-level images of annualized rates of MRI grey matter atrophy (A) and annualized rates of change of FDG-PET SUVR (B) in nfvPPA and PPAOS. Group-average voxel maps are visualized using BrainNet Viewer (https://www.nitrc.org/projects/bnv/). *T*-score maps are visualized in Fslview (https://fsl.fmrib.ox.ac.uk/fsl/fslwiki/FslView) for a better representation of both cortical and subcortical patterns. Group-average cortical regional data are visualized using the Brainnetome atlas available in the ggseg package in R (https://doi.org/10.5281/zenodo.5569249), while subcortical data are mapped from the Brainnetome onto the aseg atlas available in ggseg for visualization purposes only.

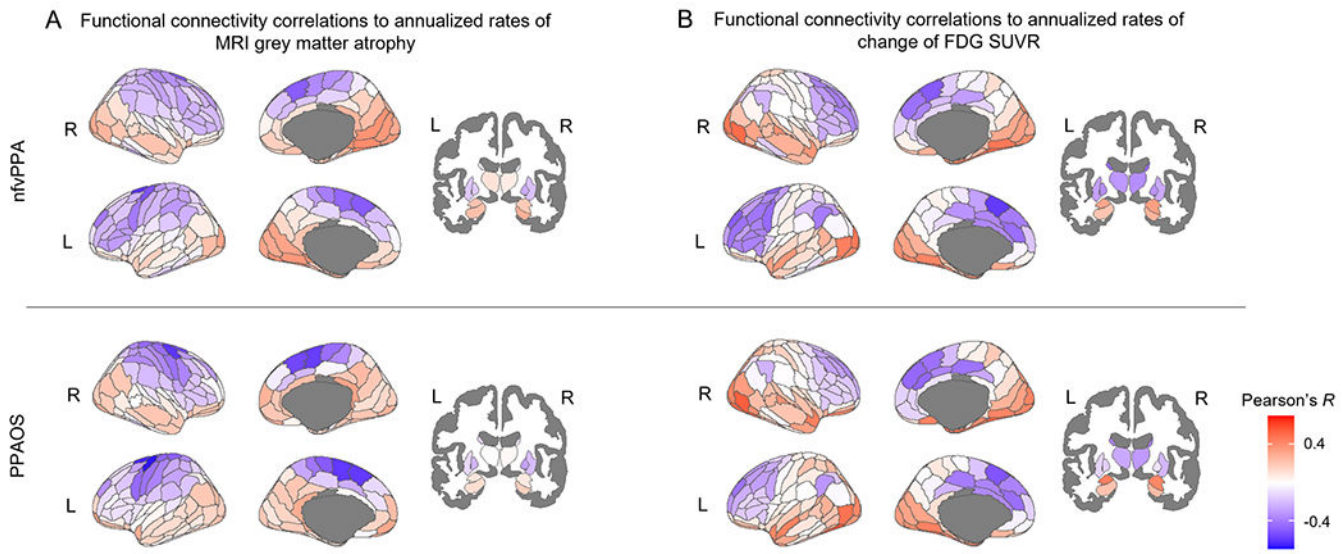

Figure 2. Correlations between baseline functional connectivity and longitudinal neurodegeneration.

Each region of the Brainnetome atlas is colored-coded based on the Pearson's *R* correlation coefficient between group-average functional connectivity from that region and measures of longitudinal rates of atrophy (A) and hypometabolism (B) in nfvPPA and PPAOS. A negative correlation (in blue) indicates that a stronger functional connectivity to the region is associated with faster rates of neurodegeneration across all other connected regions.

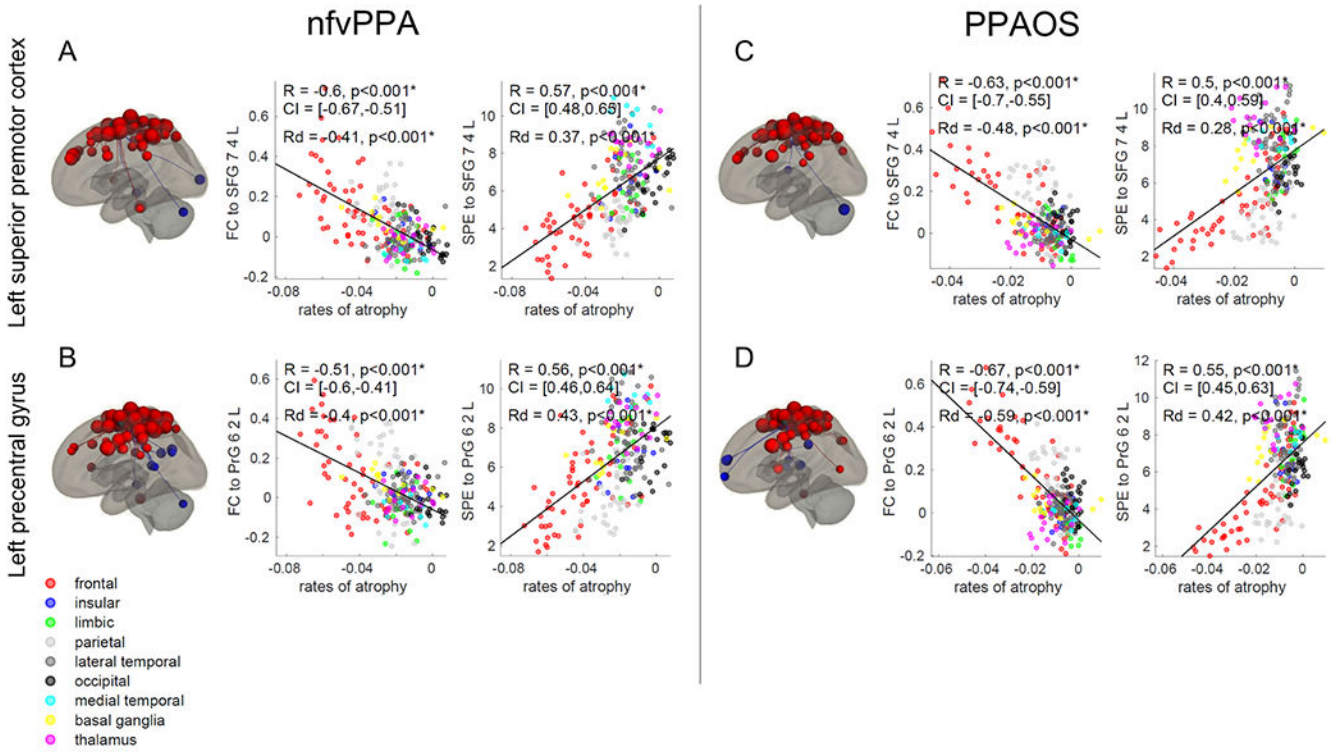

Figure 3. Epicenters' functional connectivity and rates of atrophy.

Correlations between annualized rates of MRI grey matter atrophy and functional connectivity (FC) or shortest path to the epicenter (SPE) to the dorsolateral Brodmann area 6 of left superior frontal gyrus (Brainnetome SFG_7_4_L) and the caudal dorsolateral Brodmann area 6 of the left precentral gyrus (Brainnetome PrG_6_2_L) in nfvPPA (A, B) and PPAOS (C, D). Correlations that remained statistically significant (p<0.05) after Bonferroni correction for multiple comparisons are marked with an asterisk. ROI-to-ROI functional connectivity from these regions is displayed as red dots on the brain renders (p<0.001); red dots represent functionally connected ROIs, while blue dots represent anti-correlated ROIs. R = Pearson's correlations coefficient. Rd = Pearson's partial correlations coefficient corrected for Euclidean distance from the epicenter. CI = 5%-95% confidence intervals.

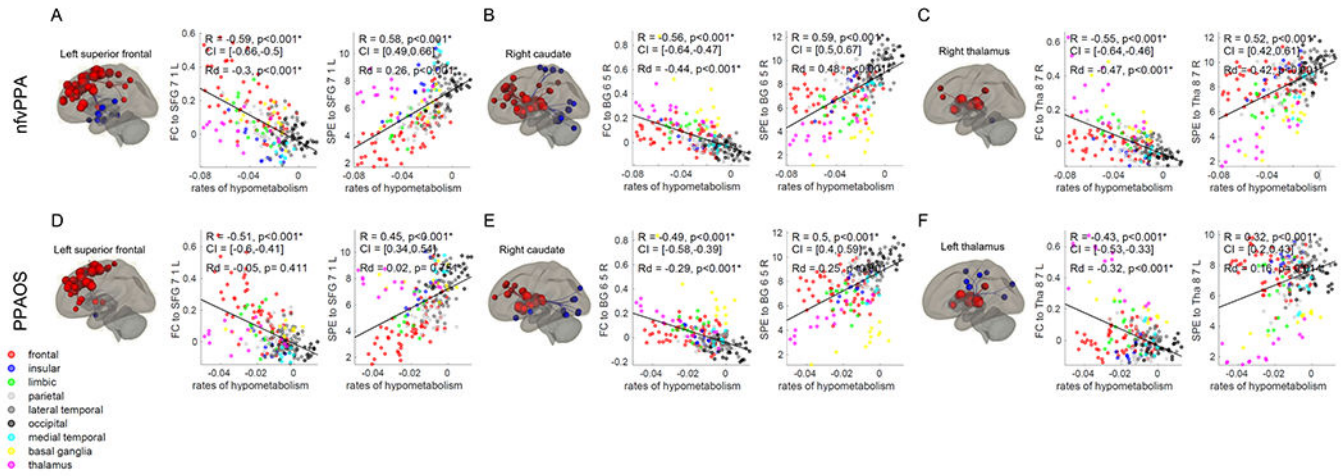

Figure 4. Epicenters' functional connectivity and rates of hypometabolism.

Correlations between annualized rates of change of FDG-PET SUVR and functional connectivity (FC) or shortest path to the epicenter (SPE) to the medial Brodmann area 8 of the superior frontal gyrus (Brainnetome SFG_7_1_L), right dorsal caudate (Brainnetome BG_6_5_R) and left and right caudal temporal thalamus (Brainnetome Tha_8_7_R and Tha_8_7_L) in nfvPPA (A, B, C) and PPAOS (D, E, F). Correlations that remained statistically significant (p<0.05) after Bonferroni correction for multiple comparisons are marked with an asterisk. ROI-to-ROI functional connectivity from these regions is displayed on brain renders (p<0.001). R = Pearson's correlations coefficient. Rd = Pearson's partial correlations coefficient corrected for Euclidean distance from the epicenter. CI = 5%-95% confidence intervals.

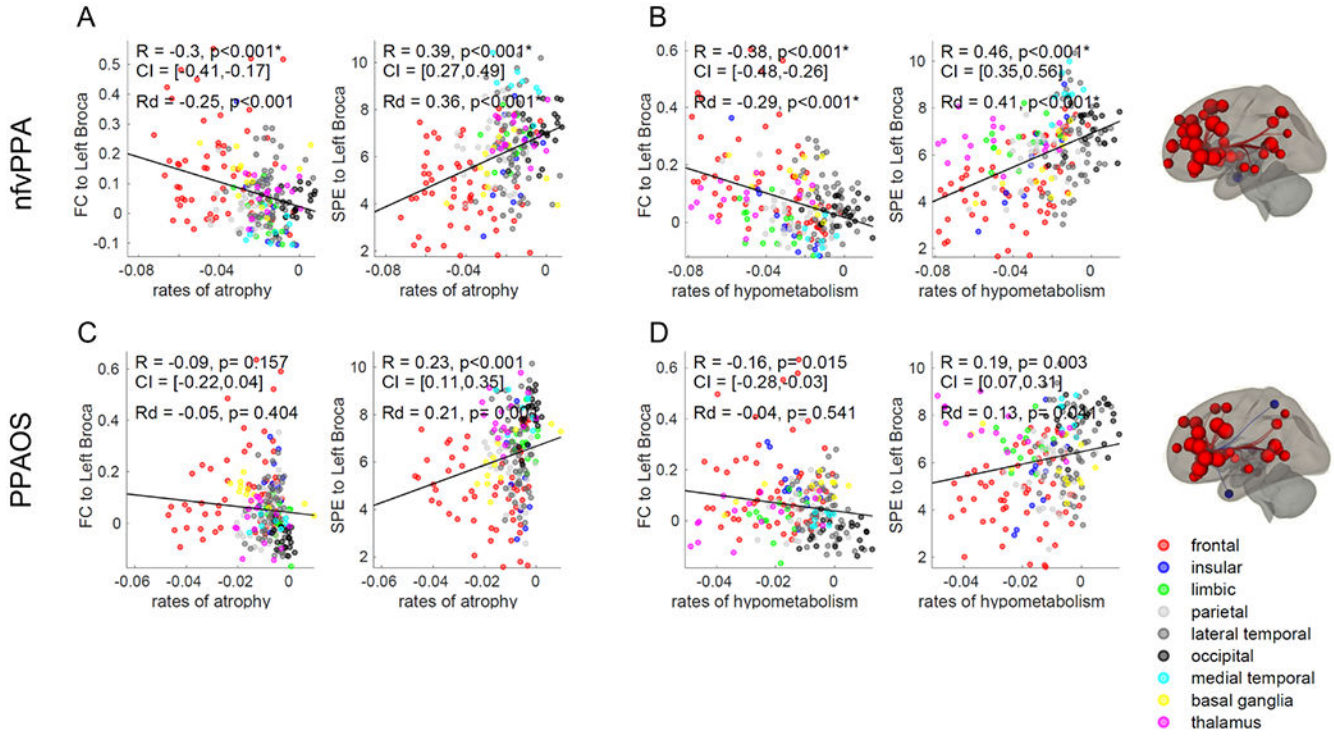

Figure 5. Functional connectivity of the left Broca's area and rates of neurodegeneration.
Correlations between annualized rates of neurodegeneration and functional connectivity (FC) or shortest path to the epicenter (SPE) to the left Broca's area in nfvPPA (A, B) and PPAOS (C, D). Correlations that remained statistically significant (p<0.05) after Bonferroni correction for multiple comparisons are marked with an asterisk. ROI-to-ROI functional connectivity from these regions is displayed on brain renders (p<0.001). R = Pearson's correlations coefficient. Rd = Pearson's partial correlations coefficient corrected for Euclidean distance from the epicenter. CI = 5%-95% confidence intervals.

Table 1:

Demographic and clinical features.

Data shown as median (inter-quartile range) or n (%). ASRS = Apraxia of Speech Rating Scale; WAB-AQ = Western Aphasia Battery – Aphasia Quotient; NAT = Northwestern Anagram Test; MDS-UPDRS III = Movement Disorders Society Sponsored Revision of the Unified Parkinson's Disease Rating Scale part III; BNT = Boston Naming Test; MSD = Motor Speech Disorder; MoCA = Montreal Cognitive Assessment Battery; FTLD-modified CDR-SB = Frontotemporal Lobar Degeneration-modified Clinical Dementia Rating – Sum of Boxes. Groupwise comparisons are from two-sample *t*-test for continuous variables and from Fisher's Exact Test for categorical variables.

		nfvPPA (n=18)	PPAOS (n=23)	
Demographics				
Female, n (%)		17 (49%)	19 (58%)	p=1
Age at baseline MRI, years		71 (64, 75)	71 (64, 78)	p=0.581
Scan interval, years		1.9 (1.3, 2.3)	2 (1.5, 2.2)	p=0.958
Estimated time from symptom onset, years		2.8 (2.4, 4.0)	3.8 (2.7, 5.4)	p=0.151
Education, years		14 (12, 16)	16 (15, 18)	p=0.029*
Neurological and neuropsychological evaluation				
ASRS3 total	Baseline	17 (12, 28)	16 (11, 22)	p=0.593
	Follow-up	28 (20, 35)	23 (18, 30)	p=0.404
WAB-AQ	Baseline	87 (81, 94)	98 (96, 100)	p<0.001 *
	Follow-up	77 (73, 83)	96 (87, 97)	p<0.001 *
NAT	Baseline	8 (6,8)	10 (9,10)	p=0.001 *
	Follow-up	5 (3,6)	9 (7,10)	p<0.001 *
MDS-UPDRS III	Baseline	16 (10, 28)	13 (5, 20)	p=0.065
	Follow-up	32 (18, 52)	31 (12, 41)	p=0.214
Token Test V	Baseline	19 (12, 20)	21 (19, 22)	p=0.001 *
	Follow-up	17 (13, 18)	20 (18, 21)	p=0.003 *
BNT	Baseline	13 (10,14)	15 (14,15)	p=0.001 *
	Follow-up	12 (10, 13)	14 (13, 15)	p<0.001 *
MSD score	Baseline	6 (5, 7)	7 (6, 8)	p=0.067
	Follow-up	4 (3, 6)	6 (4, 6)	p=0.010 *
MoCA	Baseline	24 (21, 26)	28 (26, 29)	p<0.001 *
	Follow-up	17 (14, 20)	27 (24, 28)	p<0.001 *
FTLD-modified CDR-SB	Baseline	2 (1, 3)	1 (0.63, 2)	p=0.037 *
	Follow-up	5.5 (3, 11.75)	2 (1.5, 4)	p=0.010 *
AOS subtype				
	Prosodic	4 (22%)	13 (57%)	p=0.054

			nfvPPA (n=18)	PPAOS (n=23)	
		Phonetic	7 (39%)	5 (22%)	p=0.31
		Mixed	7 (39%)	5 (22%)	p=0.31
		Dysarthria			
	Present	Baseline	3 (17%)	7 (30%)	p=1
		Follow-up	10 (56%)	13 (57%)	p=1

* PPAOS is statistically different from nfvPPA (p<0.05).